Patient-specific femoral shape estimation using a parametric model and two 2D fluoroscopic images

Yumi Iwashita†, Ryo Kurazume†, Kahori Nakamura†, Toshiyuki Okada††,
Yoshinobu Sato††, Nobuhiko Sugano††, Tsuyoshi Koyama††, and Tsutomu Hasegawa†

† Graduate Faculty of Infomation Sciencen and Electrical Engineering
Kyushu University
744 Motooka, Nishi-ku, Fukuoka, Japan

†† Graduate School of Medicine
Osaka University
2-2 Yamadaoka, Suita-shi, 565-0871, Japan

Abstract

In medical diagnostic imaging, the X-ray CT scanner and the MRI system have been widely used to examine 3D shapes and internal structures of living organisms and bones. However, these apparatuses are generally large and very expensive. Since an appointment is also required before examination, these systems are not suitable for urgent fracture diagnosis in emergency treatment. However, X-ray/fluoroscopy has been widely used as traditional medical diagnosis. Therefore, the realization of the reconstruction of precise 3D shapes of living organisms or bones from a few conventional 2D fluoroscopic images might be very useful in practice, in terms of cost, labor, and radiation exposure. The present paper proposes a method by which to estimate a patient-specific 3D shape of a femur from only two fluoroscopic images using a parametric femoral model. First, we develop a parametric femoral model by the statistical analysis of 3D femoral shapes created from CT images of 56 patients. Then, the position and shape parameters of the parametric model are estimated from two 2D fluoroscopic images using a distance map constructed by the Level Set Method. Experiments using in vivo images for hip prosthesis patients are successfully carried out, and it is verified that the proposed system has practical applications.

1. Introduction

In medical diagnostic imaging, the X-ray Computed Tomography (CT) scanner and the Magnetic Resonance Imaging (MRI) system have been widely used to examine the 3D shape or internal structure of living organisms and bones. However, these apparatuses are generally large and very expensive, and thus, they are usually installed in large medical institutions rather than small local clinics. Since an appointment is also required before examination, these systems are not suitable for urgent fracture diagnosis in emergency treatment.

However, X-ray has been widely used as traditional medical diagnosis. Recently, digital fluoroscopy has been developed and widely used in many hospitals. The cost of this fluoroscopic inspection system is much lower than that of CT or MRI systems and the system can be dealt with more conveniently. Furthermore, the risk of radiation exposure is also lower than that of the CT inspection system.

In the present paper, a technique by which to estimate the patient-specific 3D shape of a femur from only two fluoroscopic images is proposed. The proposed technique utilizes a parametric femoral model constructed by statistical analysis of 3D femoral shapes created from CT images of 56 patients. The position/attitude and shape parameters of the parametric model are then estimated from two 2D fluoroscopic images using a distance map constructed by the Level Set Method. Experiments using in vivo images for hip prosthesis patients, are successfully carried out, and it is verified that the proposed system has practical applications.

2 Related works

The 2D/3D registration problem is well established in image processing, especially for texture mapping in Computer Graphics or Augmented Reality. For a rigid object, 1) feature-based techniques [1],[2],[3], 2) image-based techniques using 3D texture, reflectance, brightness, and shading [4],[5],[6], and 3) silhouette-based techniques

[7],[8],[9],[10], have been proposed. In particular, in surgical navigation systems, Digitally Reconstructed Radiographs (DRRs) [11],[12] are widely used in 2D/3D registration for the fluoroscopy-guided surgery.

In 2D/3D registration of a non-rigid object such as soft tissues in medical imaging, similarity measure [13],[14], mutual imformation [15], affine [16],[17], geometric hashing [18], and displacement-field-based transformation [19] have been proposed and tested. In addition, the 3D shape estimation of a parameterized object, such as the shape reconstruction of mathematical plaster models with unknown parameters using a laser range finder [20], or the comparison of multiple cross-section images of a 3D model and a 3D parametric model [21], has also been studied. However, these studies assumed the use of a sufficient number of images or a precise 3D shape taken by a laser range finder, and only a few studies have examined 3D non-rigid shape reconstruction from only a few 2D images [22],[23],[24].

3 3D parametric femoral model

We utilize the statistical shape model of the femur proposed by Okada [25],[26]. In this technique, a number of 3D femoral shapes created from CT images are analyzed statistically, and the parametric femoral model [27],[28], which consists of the average 3D shape and several shape parameters, is created. With this parametric femoral model, a general 3D shape of the femur is expressed by the average shape and several shape parameters.

The concrete procedure for creating a parametric 3D femoral model is as follows:

1. Surface models of femurs are created from CT images by manual segmentation and Marching Cubes.

2. Local coordinate axes of the surface models are determined by applying the principal component analysis (PCA) to the set of 3D positions of the node points in each surface model. The Z axis is determined as the axis corresponding to the largest eigenvalue, which is toward the longitudial direction of the femoral shaft.

The region where the length from the top of the femoral head is less than 35 % of total length of the femur is extracted as a proximal femur and the center of gravity is defined as the origin of the local coordinate system.

3. One of the femoral model is selected as the reference model and displacement vector fields to all other models described by the thin plate spline are calculated using the non-rigid registration algorithm[29].

4. 1500 surface points on the reference model are selected, and their corresponding surface points on other models are determined according to the displacement vector fields. Each of the femur surface models is represented by 1500 3D positions, which is regarded as a 1500×3 dimensional shape vector. Given n shape vectors, the average shape vector is given by their average. PCA is applied to a set of the shape vectors subtracted by the average shape vector to obtain the eigenvectors whose coefficients correspond to the shape parameters.

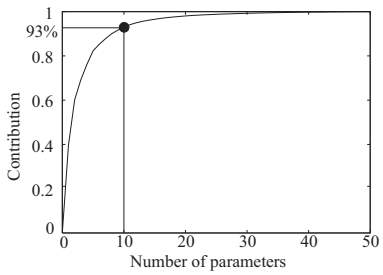

Figure 1. Contribution of parametric model

The parametric femoral model used in the following experiments was created using CT images of 56 patients. By applying PCA to 56 samples of 3D femoral shapes, we extracted the most significant 50 principal components $(p_1, p_2, \ldots, p_{50})$, standard deviation $(\sigma_1, \sigma_2, \ldots, \sigma_{50})$, and corresponding principal vectors $(v_1, v_2, \ldots, v_{50})$. With the obtained parametric femoral model, the general 3D shape of a femur is expressed as

$$x' = x + (p_1 \cdot \sigma_1 \cdot v_1) + (p_2 \cdot \sigma_2 \cdot v_2) + \cdots \quad (1)$$

where x is the surface point of the average shape and x' is the surface point of the general shape. Therefore, the general 3D shape of a femur is expressed by the parametric femoral model with

- average 3D shape and several principal vectors (predetermined)
- several (up to 50) shape parameters (estimated)

Figure 1 shows the contribution ratio of the shape parameters for the statistical femoral model.

4. Reconstruction of 3D femoral shape from two 2D fluoroscopic images

In this section, we introduce the 2D/3D registration algorithm and the estimation procedure of the optimum shape parameters using two fluoroscopic images.

This 2D/3D registration algorithm utilizes the contour lines of the silhouette of the 2D image and the projected contour lines of the 3D model. The optimum position of the

3D model is determined such that the contour lines coincide with each other on the 2D image plane. In commonly used approaches such as the ICP algorithm, the error metric is usually defined as the sum of the distances between the points on the 2D contour lines and their nearest points on the projected contour lines of the 3D model. However, the nearest point search is a laborious task and is time consuming even for the kd tree-based algorithm [30].

In the present approach, the 2D distance map [7] is utilized. First, the 2D distance map from the contour lines is created on the 2D image using the Fast Marching Method [31],[32] or raster scan algorithms [33]. Once the 2D distance map is created, the error metric is obtained directly from the 2D distance map as the value at the points on the projected contour lines of the 3D model. Using the course-to-fine strategy called "Distance Band" [7], a 2D distance map can be constructed quite rapidly using the Fast Marching Method.

After creating the 2D distance map, the parametric femoral model is placed at an arbitrary position and the 2D projection image of the 3D model is calculated. Then, contour lines of the projected image and corresponding 3D patches of the 3D model are extracted. Finally, the force which is calculated from the 2D distance map at the projected contour points is applyed directly to the corresponding 3D patch, and the optimum position and the shape parameters are estimated as shown in Fig.3.

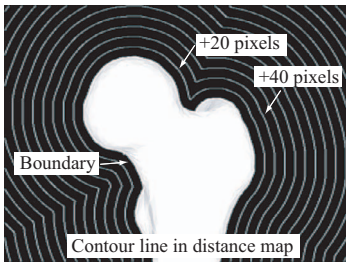

Figure 2. 2D distance map from contour in the femoral image

5 In vivo experiments

We conducted in vivo experiments for hip prosthesis patients. Fluoroscopic images of four patients were taken in clinical practice using the fluoroscopic imaging apparatus (Siemens, Siremobil ISO-C), and shapes measured by the CT scanner and estimated by parameter estimation were compared.

5.1 Calibration procedure

First, we measured the internal and external parameters. A non-coplanar marker and a coplanar marker, shown in Fig.4, are used for the calibration of external and internal parameters, respectively. These markers are constructed of acrylonitrile butadiene styrene (ABS), which indicated the highest transmission of X-rays in preliminary experimentation. The non-coplanar marker contains nine small stainless steel spheres and the coplanar marker contains 16 small stainless steel disks. The calibration procedure using these markers is as follows:

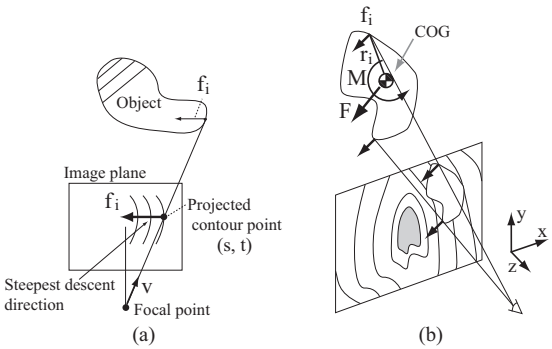

Figure 3. Calculation of the total force and moment around the COG

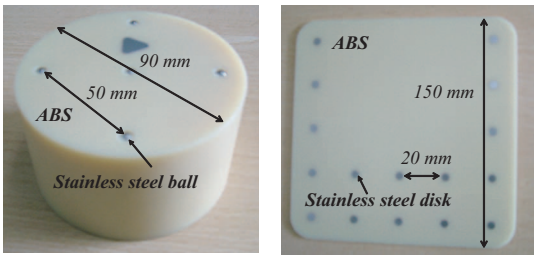

Figure 4. Non-coplanar and coplanar markers

step 1. The non-coplanar marker is captured by X-ray CT and the relative positions of the stainless steel spheres

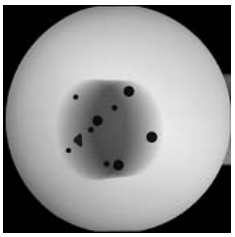

Figure 5. Example fluoroscopic image of non-coplanar marker

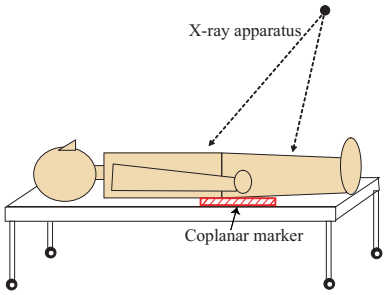

Figure 6. X-ray photography of coplanar marker

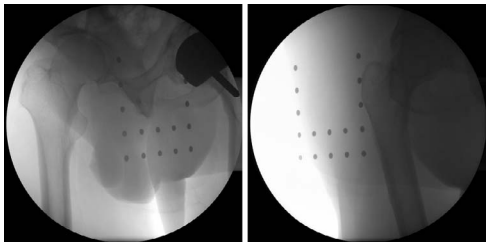

Figure 7. Two fluoroscopic femoral images of hip prosthesis patients

are measured.

step 2. A fluoroscopic image of the non-coplanar marker is captured, as shown in Fig.5, and the internal parameters of the fluoroscopic imaging apparatus are estimated by Tsai's method.

step 3. The coplanar marker is placed under the patient's hip and two fluoroscopic images of the femur are captured from two directions, as shown in Figs.6,7.

step 4. The external parameters of two fluoroscopic images are estimated using the internal parameters obtained in Step 2 and the projection image of stainless steel disks by Tsai's method.

Figure 8. Extracted contours of the femur in fluoroscopic images

5.2 Results

First, we manually extracted the contour of the femur (Fig.8) in the fluoroscopic images (Fig.7). Image size and resolution are 512 × 512 pixels and 0.454 mm/pixel. We then estimated the position and 10 shape parameters from the silhouette of the femur. The precise 3D shapes of patients' femurs were measured precisely by CT scanner.

The average errors and standard deviations of the estimated femoral shapes are shown in Fig.9. In these figures, "0" in the horizontal axis shows the case in which only the position is estimated without parameter estimation.

The experimental results show that the average error between the estimated shape and the actual shape is approximately 0.8 mm to 1.1 mm for the in vivo experiments. One example of average, actual, and estimated shapes for Case 4 is shown in Fig.10, and the distribution of average error is shown in Fig.11. In Fig.11, dark regions indicate less error, and the brightness of each point is proportional to its average error. From this figure, we verified that the errors in the femoral head and lesser trochanter are reduced.

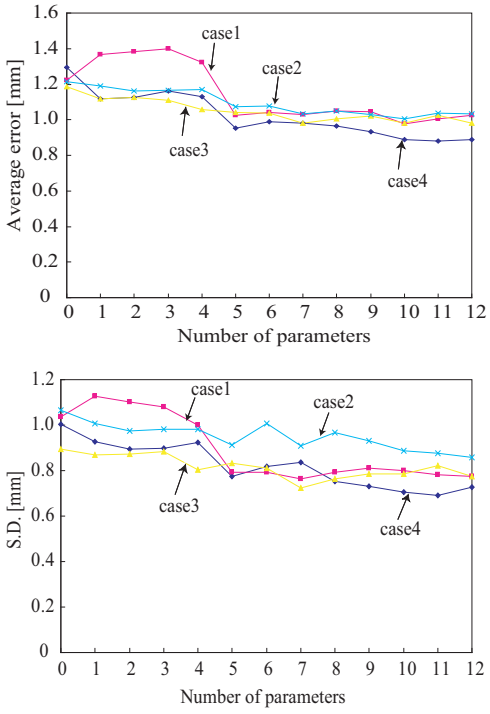

Figure 9. Average error and standard deviation for the number of estimated shape parameters for the femurs of four patients

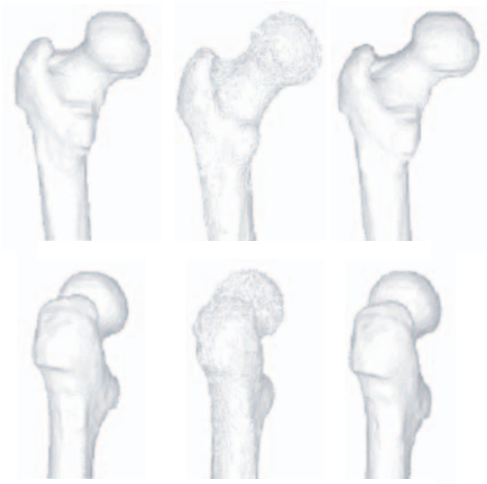

Initial shape Estimated shape Actual shape

Figure 10. Actual and estimated femoral model with and without shape parameter estimation for Case 4

0 5 10

Number of parameters

Figure 11. Error distribution indicated by brightness (higher brightness indicates larger error

6 Conclusions

We proposed a method by which to estimate the 3D shape of the in vivo femur from only two fluoroscopic images using a parametric femoral model. Although the precise 3D shape of the femur is usually measured using a CT scanner or an MRI system, the proposed method enables a precise 3D shape to be estimated using only two fluoroscopic images taken by an inexpensive fluoroscopic inspection apparatus. Thus, the cost of the inspection system can be dramatically reduced and the 3D image-based medical diagnosis becomes available even in small clinics.

In vivo experiments revealed the average error between the estimated shape and the actual shape to be 0.8 mm to 1.1 mm, and it was verified that the 3D shape can be estimated using two 2D fluoroscopic images taken from different view points with the same accuracy as in the case of 3D shapes being compared directly.

References

[1] I. Stamos and P. K. Allen. Integration of range and image sensing for photorealistic 3d modeling. In *Proc. of the 2000 IEEE International Conference on Robotics and Automation*, pp. 1435–1440, 2000.

[2] I. Stamos and P. K. Allen. Automatic registration of 2-d with 3-d imagery in urban environments. In *Proc. of the International Conference on Computer Vision*, pp. 731–737, 2001.

[3] L. Liu and I. Stamos. Automatic 3d to 2d registration for the photorealistic rendering of urban scenes. In *IEEE International Conference on Robotics & Automation*, 2005.

[4] R. Kurazume, K. Noshino, Z. Zhang, and K. Ikeuchi. Simultaneous 2d images and 3d geometric model registration for texture mapping utilizing reflectance attribute. In *Proc. of Fifth Asian Conference on Computer Vision (ACCV)*, pp. 99—106, 2002.

[5] M. D. Elstrom and P. W. Smith. Stereo-based registration of multi-sensor imagery for enhanced visualization of remote environments. In *Proc. of the 1999 IEEE International Conference on Robotics and Automation*, pp. 1948–1953, 1999.

[6] K. Umeda, G. Godin, and M. Rioux. Registration of range and color images using gradient constraints and range intensity images. In *Proc. of 17th International Conference on Pattern Recognition*, pp. 12–15, 2004.

[7] Y. Iwashita, R. Kurazume, K. Hara, and T. Hasegawa, Fast Alignment of 3D Geometrical Models and 2D Color Images using 2D Distance Maps, in *Proc. The 5th International Conference on 3-D Digital Imaging and Modeling (3DIM)*, pp.164-171, 2005.

[8] Q. Delamarre and O. Faugeras. 3d articulated models and multi-view tracking with silhouettes. In *Proc. of the International Conference on Computer Vision*, Vol. 2, pp. 716–721, 1999.

[9] K. Matsushita and T. Kaneko. Efficient and handy texture mapping on 3d surfaces. In *Comput. Graphics Forum 18*, pp. 349–358, 1999.

[10] P. J. Neugebauer and K. Klein. Texturing 3d models of real world objects from multiple unregistered photographic views. In *Computer Graphics Forum 18*, pp. 245–256, 1999.

[11] G. Penny, J. Weese, J. Little, P. Desmedt, D. Hill, and D. Hawkes, A Comparison of Similarity Measures for Use in 2-D/3-D Medical Image Registration, IEEE Trans. Medical Imaging, Vol.17, No.4, pp.586-595, 1998.

[12] L. Zollei, E. Grimson, A. Norbash, and W. Wells, 2D-3D rigid registration of x-ray fluoroscopy and CT images using mutual information and sparsely sampled histogram estimators, In *Proc. of Computer Vision and Pattern Recognition*, pp.696–703, 2001.

[13] C. V. Stewart, C. L. Tsai, and A. Perera. A view-based approach to registration: Theory and application to vascular image regisrtaion. In *International Conference on Information Processing in Medical Imaging (IPMI)*, pp. 475–486, 2003.

[14] A. Guimond, A. Roche,M. Ayache, and J. Meunier. Three-dimensional multimodal brain warping using the demons algorithm and adaptive intensity corrections. *IEEE Transaction on Medical Imaging*, Vol. 20, No. 1, pp. 58–69, 2001.

[15] F. Maes, A. Collignon, D. Vandermeulen, G. Marchal, and P. Suetens. Multimodality image registration by maximization of mutual infomation. *IEEE Transaction on Medical Imaging*, Vol. 16, No. 2, pp. 187–198, 1997.

[16] C. V. Stewart, C. L. Tsai, and A. Perera. Rigid and affine registration of smooth surfaces using differential properties. Proc. of Third European Conference on Computer Vision (ECCV'94), pp. 397–406, 1994.

[17] C. R. Meyer, J. L. Boes, B. Kim, P. H. Bland, K. R. Zasadny, P. V. Kison, K. Korak, K. A. Fery, and R. L. Wahl. Demonstration of accuracy and clinical versatility of mutual information for automatic multimodality image fusion using affine and thin plate spline warped geometric deformations. *Medical Image Analysis*, Vol. 1, No. 3, pp.195–206, 1997.

[18] A. Gueziec, X. Pennec, and N. Ayache. Medical image registration using geometric hashing. *IEEE Computational Science and Engineering, special issue on Geometric Hashing*, Vol. 4, No. 4, pp. 29–41, 1997.

[19] P. R. Andresen and M. Nielsen. Non-rigid registration by geometry constrained diffusion. Medical Image Computing and Computer-Assisted Intervention(MICCAI' 99), pp. 533–543, 1999.

[20] T. Masuda, Y. Hirota, K. Ikeuchi, and K. Nishino. Simultaneous determination of registration and deformation parameters among 3d range images. In *Fifth International Conference on 3-D Digital Imaging and Modeling*, pp. 369–376, 2005.

[21] CSK Chan, DC Barratt, PJ Edwards, GP Penney, M Slomczykowski, TJ Charter, and DJ Hawkes. Cadaver validation of the use of ultrasound for 3d model instantiation of bony anatomy in image guided orthopaedic surgery. In *Lecture Notes in Computer Science, 3217 (Proc. 7th International Conference on Medical Image Computing and Computer Assisted Intervention, Part II (MICCAI 2004), St-Malo, France)*, pp. 397–404, 2004.

[22] D. Terzopoulos and D. Metaxas, Dynamic 3D Models with Local and Global Deformations: Deformable Superquadrics, *IEEE Trans. on Pattern Analysis and Machine Intelligence*, Vol 13, No.7, pp.703-714, 1991.

[23] K. Nakamura, R. Kurazume, T. Okada, Y. Sato, N. Sugano, and T. Hasegawa, 3D reconstruction of a femoral shape using a parametric model and two 2D radiographs In *Proc. of Meeting on Image Recognition and Understanding*, pp.78-83, 2006.

[24] G. Zheng, M. Ballester, M. Styner, and L. Nolte, Reconstruction of Patient-specific 3D Bone Surface from 2D Calibrated Fluoroscopic Images and Point Distribution Model In *Proc. of Medical Image Computing and Computer-Assisted Intervention(MICCAI'06)*, pp.25-32, 2006.

[25] Keita Yokota and Toshiyuki Okada and Masahiko Nakamoto and Yoshinobu Sato and Masatoshi Hori and J. Masumoto and Hironobu Nakamura and Shinichi Tamura, "Construction of conditional statistical atlases of the liver based on spatial normalization using surrounding structures", *International Journal of Computer Assisted Radiology and Surgery*, pp. 39-40, 2006,

[26] Toshiyuki Okada and Ryuji Shimada and Yoshinobu Sato and Masatoshi Hori and Keita Yokota and Masahiko Nakamoto and Yen-Wei Chen and Hironobu Nakamura and Shinichi Tamura, "Automated segmentation of the liver from 3D CT images using probabilistic atlas and multi-level statistical shape model", *Proceedings of the 10th International Conference on Medical Image Computing and Computer Assisted Intervention (Proc. MICCAI 2007)*, in press, 2007

[27] TF Cootes TF, CJ Cooper, CJ Taylor, and J Graham. Active shape models — their training and application,. *Computer Vision and Image Understanding*, Vol. 61, No. 1, pp. 38–59, 1995.

[28] T. Okada, M. Nakamoto, Y. Sato, N. Sugano, H. Yoshikawa, S. Tamura, T. Asaka, Y.-W. Chen, Effects of surface correspondence methods in statistical shape modelling of the proximal femur on approximation accuracy In *Proc. of the 20th International Congress and Exhibition, Computer Assisted Radiology and Surgery CARS 2006*, 016, 2006.

[29] Haili Chui and Anand Rangarajan, "A new point matching algorithm for non-rigid registration", *Computer Vision and Image Understanding*, Vol 89, No. 2-3, pp 114-141, 2003.

[30] M. Greenspan, M. Yurick, Approximate k-d tree search for efficient ICP, in *Proc. of 3-D Digital Imaging and Modeling (3DIM) 2003* pp.442–448, 2003.

[31] J. Sethian. *Level Set Methods and Fast Marching Methods, second edition*. Cambridge University Press, UK, 1999.

[32] J. Sethian. A fast marching level set method for monotonically advancing fronts. In *Proc. of the National Academy of Science*, Vol. 93, pp. 1591–1595, 1996.

[33] S. W. Shih and Y. T. Wu, Fast Euclidean distance transformation in two scans using a 3 3 neighborhood, Computer Vision and Image Understanding, Vol.93, No.2, pp.195–205, 2004.

[34] R. Y. Tsai, An Efficient and Accurate Camera Calibration Technique for 3D Machine Vision, in *Proc. of IEEE Conference on Computer Vision and Pattern Recognition*, pp. 364-374, 1986.